ELSEVIER

Materials Science and Engineering A327 (2002) 76–79

MATERIALS SCIENCE & ENGINEERING A

www.elsevier.com/locate/msea

Effect of stress relief temperature and cooling rate on pressure vessel steel welds

M.K. Miller [a,*], S.S. Babu [b], M.A. Sokolov [c], R.K. Nanstad [c], S.K. Iskander [c]

[a] *Microscopy and Microanalytical Sciences Group, Metals and Ceramics Division, Oak Ridge National Laboratory, P.O. Box 2008, Building 5500, Oak Ridge, TN 37831-6136, USA*

[b] *Materials Joining and Nondestructive Testing Group, Metals and Ceramics Division, Oak Ridge National Laboratory, Oak Ridge, TN 37831-6096, USA*

[c] *Fracture Mechanics Group, Metals and Ceramics Division, Oak Ridge National Laboratory, Oak Ridge, TN 37831-6151, USA*

Abstract

The compositions of the matrices of welds in a pressure vessel steel have been determined by atom probe tomography after a series of stress relief treatments. The weld had a bulk composition of Fe–0.29 at.% Cu–1.69 at.% Mn–0.54 at.% Ni–0.69 at.% Si–0.25 at.% Mo–0.08 at.% Cr–0.38 at.% C–0.022 at.% P–0.017 at.% S and was characterized in the as-welded state, after stress relief treatments of 24 h at 650 °C, 24 h at 610 °C, and 100 h at 580 °C followed by slow cooling to room temperature and after 24 h at 650 °C and 24 h at 610 °C followed by fast cooling to room temperature. Lower stress relief temperatures and slower cooling of the material from the stress relief temperature to room temperature both reduce the copper level in the matrix and should lead to less embrittlement during service in a nuclear reactor. Published by Elsevier Science B.V.

Keywords: Pressure vessel steel; Welds; Atom probe; Ductility

1. Introduction

The copper content of welds in pressure vessels is one of the key parameters that determine the amount of embrittlement that occurs during service in a nuclear reactor. Atom probe field ion microscopy has established that the copper that remains in the matrix after the stress relief treatment forms a high density of ultrafine body centered cubic copper-enriched precipitates that are also enriched in nickel, manganese, silicon and phosphorus [1–7]. These copper precipitates are one of the primary microstructural features that cause embrittlement. Extrapolation of high temperature solubility data and thermodynamic predictions indicate that the solubility of copper in the matrix changes relatively rapidly over the temperature range ($\sim$575 to $\sim$650 °C) that is normally used to relieve the stresses in the pressure vessel before service. Therefore, the temperature and the cooling rate after stress relief treatment should influence the level of copper in the matrix and hence the degree of embrittlement. In this paper, the influence of these parameters on the copper level in the matrix has been investigated by atom probe tomography [8].

2. Experimental

The high copper weld (test plate 002 A with a Linde 80 flux) used in this study has a bulk composition of Fe–0.29 at.% Cu–1.69 at.% Mn–0.54 at.% Ni–0.69 at.% Si–0.25 at.% Mo–0.08 at.% Cr–0.38 at.% C–0.022 at.% P and 0.017 at.% S. The material was characterized in the as-welded state and after the following three heat treatments: (A) 24 h at 650 °C; (B) 24 h at 610 °C; and (C) 100 h at 580 °C. The temperatures were controlled to a level of ± 2 °C. Following each of these isothermal heat treatments, the material was slow cooled at a rate of 8 °C h^{-1} to room temperature (25 °C). This cooling rate is typical of that experienced by a 150 mm-thick section of a pressure vessel. In order to evaluate the influence of the cooling rate after the stress relief treatment, some material was examined after heat treatments of 24 h at 650 °C and 24 h at

* Corresponding author. Tel.: +1-865-574-4719; fax: +1-865-241-3650.

E-mail address: millermk@ornl.gov (M.K. Miller).

0921-5093/02/$ - see front matter. Published by Elsevier Science B.V.
PII: S0921-5093(01)01879-2

Table 1
Thermodynamic predictions of the compositions of the co-existing phases at different temperatures

at.%		Cr	Ni	Si	Mo	Mn	Cu	Fe
Bulk		0.08	0.54	0.69	0.25	1.69	0.291	Balance
650 °C	Matrix	0.08	0.54	0.69	0.25	1.69	0.290	Balance
	ε-cu	Not present						
610 °C	Matrix	0.08	0.54	0.69	0.25	1.69	0.248	Balance
	ε-cu	0.00	0.54	0.00	0.81	4.22	94.121	0.30
580 °C	Matrix	0.08	0.54	0.69	0.25	1.69	0.185	Balance
	ε-cu	0.00	0.59	0.00	0.90	4.69	93.579	0.24
454 °C	Matrix	0.08	0.54	0.69	0.25	1.68	0.046	Balance
	ε-cu	0.00	0.93	0.00	1.50	7.09	90.403	0.08

610 °C followed by water quenching to room temperature. In order to evaluate the effect of a typical post-irradiation treatment, some material was also examined after a heat treatment of 24 h at 610 °C, slow cooled to room temperature and 168 h at 454 °C and slow cooled to room temperature.

The subsize Charpy specimens were tested on a specially modified pendulum-type instrumented impact machine. Specimens have a length of 25.4 mm (1 in.), 3 by 4-mm cross-section, with a 60° notch 1 mm deep and a root radius of 0.1 mm. The span (i.e. the minimum distance between the radii of the anvils) was 20 mm. The ductile-to-brittle transition temperature (DBTT) was determined at the half of the upper shelf.

The composition of the matrix of each of these heat treatments was determined in an energy-compensated optical position-sensitive atom probe [8]. The experimental conditions used for atom probe analysis were a specimen temperature of 50 K, a 20% pulse fraction and a pulse repetition rate of 1500 Hz.

3. Thermodynamic predictions

The predicted equilibrium compositions of the co-existing phases were determined with the use of Thermocalc™ version M and the SSOL database. In these calculations, the alloy composition was Fe–0.29 at.% Cu–1.69 at.% Mn–0.54 at.% Ni–0.69 at.% Si–0.25 at.% Mo–0.08 at.% Cr. The results of the thermodynamic predictions are summarized in Table 1. These predictions indicate that the copper in the material is lower than the solubility limit at 650 °C of the body centered cubic ferrite matrix and no face centered cubic ε-copper precipitates are formed. The ε-copper precipitates were predicted to form at 626 °C and lower temperatures for this alloy composition. As expected, the copper content of the ferrite matrix decreases with decreasing temperature, as shown in Fig. 1. The curvature of the phase boundary in the temperature range 500–650 °C indicates that small changes in the temperature will significantly influence the level of copper in solution in the matrix. The manganese, nickel, silicon, molybdenum and chromium contents of the matrix do not change significantly with temperature.

The copper and iron contents of the ε-copper precipitates were also predicted to decrease and the manganese, nickel and molybdenum levels increase with decreasing temperature. No silicon or chromium solubility was predicted for the ε-copper precipitates.

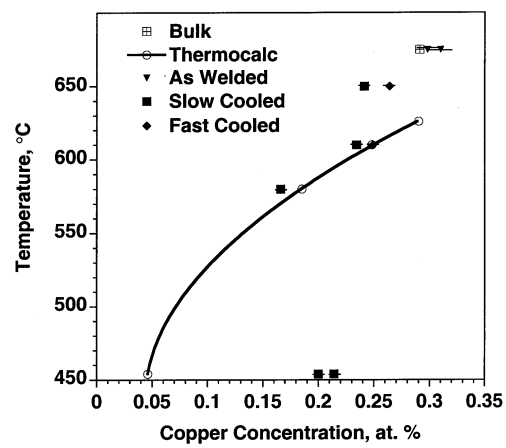

Fig. 1. The predicted and measured copper concentrations of the matrix after different stress relief treatments.

Table 2
Transition temperatures of the different heat treatments

Heat treatment	Transition temperature (°C)
24 h at 650 °C, slow cooled	−55
24 h at 610 °C, slow cooled	−55
100 h at 580 °C, slow cooled	−51
24 h at 610 °C, fast cooled	−72
24 h at 610 °C, slow cooled + 168 h at 454 °C	−37

4. Results and discussion

The transition temperature results of the different heat treatments are given in Table 2. No significant differences were found in the transition temperature among the materials annealed for 24 h at 650 °C, 24 h at 610 °C and 100 h at 580 °C and slow cooled to room temperature. These results are consistent with those from similar pressure vessel steels in the embrittlement database (EDB) of mechanical properties [9]. Annealing the 610 °C material for the additional 168 h at 454 °C produced an unexpected small increase in the transition temperature and a previously observed increase in the upper shelf energy [10].

The results of the measured copper concentrations in the matrix of this weld are shown in Fig. 1. For ease of representation, the temperatures used in this plot for the slow cooled materials are the isothermal annealing temperatures. However, it should be noted that significant time is spent at lower temperatures. In addition, the bulk copper level in the as-welded material was measured by the traditional chemical methods and the copper level in the matrix of the as-welded material was measured by the atom probe and are included in Fig. 1.

The copper content in the matrix of the as-welded material was found to be slightly higher than the bulk composition. This small increase is due to the presence of coarse carbides, which have little or no copper solubility. A small reduction from the bulk copper level was measured in the matrix of the material aged for 24 h at 650 °C and water quenched. This result indicates that high stress relief temperatures (≥ 625 °C) are not effective in significantly reducing the matrix copper levels in high copper welds (i.e. greater than 0.29 at.% Cu). The copper content in the matrix of the material aged for 24 h at 610 °C and fast cooled to room temperature was slightly lower than that of the similar 650 °C annealed material and the copper level was in excellent agreement with the thermodynamic prediction. In accordance with the thermodynamic predictions and the phase diagram, it is evident that a lower stress relief temperature reduces the copper in solution in the matrix and therefore the amount of copper available for the formation of copper-enriched precipitates during neutron irradiation.

A comparison of the fast and slow cooled conditions at 650 °C reveals that the copper level in the matrix is significantly lower in the slow cooled materials. In addition, the copper levels in all the three slow cooled materials were lower than the thermodynamic predictions for the isothermal annealing temperatures. These decreases are due to the additional time spent at elevated temperature during slow cooling while significant solute diffusion and precipitation of ε-copper can occur. As the copper found in the matrix of this type of steel after neutron irradiation to a fluence of $\sim 2 \times 10^{23}$ m^{-2} is typically ~ 0.05 at.% Cu, the slow cooling reduces the amount of copper available in the matrix to form body centred cubic copper-enriched precipitates by ~ 15 and ~ 7% for the 650 and 610 °C materials, respectively. Consequently, this lower copper level will also reduce the amount of embrittlement due to the lower number density of copper-enriched precipitates. It is therefore important to take the full heat treatment into account when comparing embrittlement data. Interpretation of data from the EDB should be based on the matrix copper concentration rather than the bulk copper content for pressure vessel steels with copper contents greater than the solubility limit at the effective stress relief temperature.

A comparison of the material annealed for the typical post-irradiation treatment of 168 h at 454 °C to the material annealed at 24 h at 610 °C reveals a small but beneficial decrease in the copper level in the matrix. As the measured copper content was significantly higher than the thermodynamic prediction, the 168 h at 454 °C was insufficient to reach the equilibrium composition due to the low diffusion rates at this low temperature.

5. Conclusions

This atom probe tomography study has demonstrated that a lower stress relief temperature and slow cooling the material from the stress relief temperature to room temperature both reduce the copper level in the matrix of pressure vessel steels. This lower matrix copper level will consequently decrease the number of copper-enriched precipitates that form during irradiation and thereby the level of embrittlement of the steel.

Acknowledgements

The authors thank K.F. Russell for her technical assistance. The research at the Oak Ridge National Laboratory SHaRE User Facility was sponsored by the Division of Materials Sciences and Engineering, US Department of Energy, and by the Office of Nuclear Regulatory Research, US Nuclear Regulatory Commission under inter-agency agreement DOE 1886-N695-3W with the US Department of Energy, under contract DE-AC05-00OR22725 with UT-Battelle, LLC.

References

[1] M.K. Miller, P. Pareige, M.G. Burke, Mater. Char. (2001) 235–254.
[2] M.K. Miller, M.G. Hetherington, M.G. Burke, Metall. Trans. 20A (1989) 2651–2661.

[3] M.K. Miller, M.G. Burke, in: N.H. Packan, R.E. Stoller, A.S. Kumar (Eds.), Proceedings of the 14th International Symposium on Effects of Radiation on Materials, ASTM-STP 1046, vol. 2, American Society for Testing and Materials, Philadelphia, PA, 1990, pp. 107–126.
[4] M.K. Miller, M.G. Burke, J. Nucl. Mater. 195 (1992) 68–82.
[5] P. Pareige, R.E. Stoller, K.F. Russell, M.K. Miller, J. Nucl. Mater. 249 (1997) 165–174.
[6] M.K. Miller, K.F. Russell, J. Nucl. Mater. 250 (1997) 223–228.
[7] P. Pareige, K.F. Russell, R.E. Stoller, M.K. Miller, J. Nucl. Mater. 250 (1997) 176–183.
[8] M.K. Miller, Atom Probe Tomography: Analysis at the Atomic Level, Kluwer Academic/Plenum Press, Dordrecht/New York, 2000.
[9] J.A. Wang, F.B.K. Kam, F.W. Stallmann, in: D.S. Gelles, R.K. Nanstad, A.S. Kumar, E.A. Little (Eds.), Effects of Radiation on Materials, ASTM STP 1270, American Society of Testing and Materials, West Conshohocken, PA, 1996, pp. 500–521 (J.A. Wang, Embrittlement Data Base, Version 1: NUREG/CR-6506, ORNL/TM-13327, 1997).
[10] S.K. Islander, M.A. Sokolov, R.K. Nanstad, in: R.K. Nanstad, M.L. Hamilton, F.A. Garner, A.S. Kumar (Eds.), Proceedings of the 18th International Symposium on Effects of Radiation on Materials, ASTM STP 1325, American Society of Testing and Materials, West Conshohocken, PA, 1999, pp. 403–420.